

Falkland Islands Fisheries Department

***Loligo* Stock Assessment, Second Season 2013**

Andreas Winter

November 2013

Index

Summary	3
Introduction.....	3
Methods.....	5
Stock assessment.....	7
Data.....	7
Group arrivals / depletion criteria.....	9
Depletion analyses	12
South.....	12
North.....	13
Escapement biomass.....	14
Immigration	15
References.....	16
Appendix A.....	18
Appendix B.....	19
Appendix C.....	21
Appendix D.....	22

Summary

- 1) The second season *Loligo* fishery of 2013 was open for the scheduled 78 days from July 15th to September 30th. 19,614 tonnes of *Doryteuthis gahi* catch were reported; a total that is below average compared to previous second seasons. In the Loligo Box 60.7% of *D. gahi* catch and 58.9% of effort were taken south of 52° S; 39.3% of *D. gahi* catch and 41.1% of effort were taken north of 52° S.
- 2) Sub-areas north and south of 52° S were depletion-modelled separately. In the north sub-area, four in-season depletion periods were inferred to have started on July 19th, August 14th, September 8th, and September 23rd. In the south sub-area, three in-season depletion periods were inferred to have started on July 21st, August 17th, and September 8th.
- 3) Approximately 9,500 tonnes of *D. gahi* (95% confidence interval: [1,041 to 32,173] tonnes) were estimated to have immigrated into the Loligo Box during second season 2013, representing 21% of the *D. gahi* biomass in the fishing zone.
- 4) The final total estimate for *D. gahi* remaining in the Loligo Box at the end of second season 2013 was:
Maximum likelihood of 25,500 tonnes, with a 95% confidence interval of [19,014 to 48,197] tonnes.
The risk of *D. gahi* escapement biomass at the end of the season being less than 10,000 tonnes was estimated at effectively zero.

Introduction

The second season of the 2013 *Loligo* fishery (*Doryteuthis gahi* – Patagonian squid) started on July 15th, and ended by directed closure on September 30th. Total reported *D. gahi* catch by X-licensed vessels was 19,614 tonnes; making 2013 the first year on record since 2004 in which 2nd season catch was less than 1st season catch (Table 1).

Table 1. *D. gahi* season catch and effort since 2004. Days: total number of calendar days open to C / X-licensed fishing including (since 1st season 2013) extension days; Vessel Days: aggregate number of licensed *D. gahi* fishing days reported by all vessels for the season.

	Season 1			Season 2		
	Catch (t)	Days	Vessel Days	Catch (t)	Days	Vessel Days
2004				17,559	78	1271
2005	24,605	45	576	29,659	78	1210
2006	19,056	50	704	23,238	53	883
2007	17,229	50	680	24,171	63	1063
2008	24,752	51	780	26,996	78	1189
2009	12,764	50	773	17,836	59	923
2010	28,754	50	765	36,993	78	1169
2011	15,271	50	771	18,725	70	1099
2012	34,767	51	770	35,026	78	1095
2013	19,908	53	782	19,614	78	1195

As in previous seasons, the *D. gahi* stock assessment was conducted with depletion time-series models (Agnew et al., 1998; Roa-Ureta and Arkhipkin, 2007;

Arkhipkin et al., 2008). Because *D. gahi* has an annual life cycle (Patterson, 1988), stock cannot be derived from a standing biomass carried over from prior years (Rosenberg et al., 1990). The depletion model instead calculates an estimate of population abundance over time by evaluating what levels of abundance and catchability must be extant to sustain the observed rate of catch. Depletion modelling is used both in-season and for the post-season summary, with the objective of maintaining an escapement biomass of 10,000 tonnes *D. gahi* at the end of each season as a conservation threshold (Agnew et al., 2002; Barton, 2002).

Survey, 30/06 - 14/07 2013

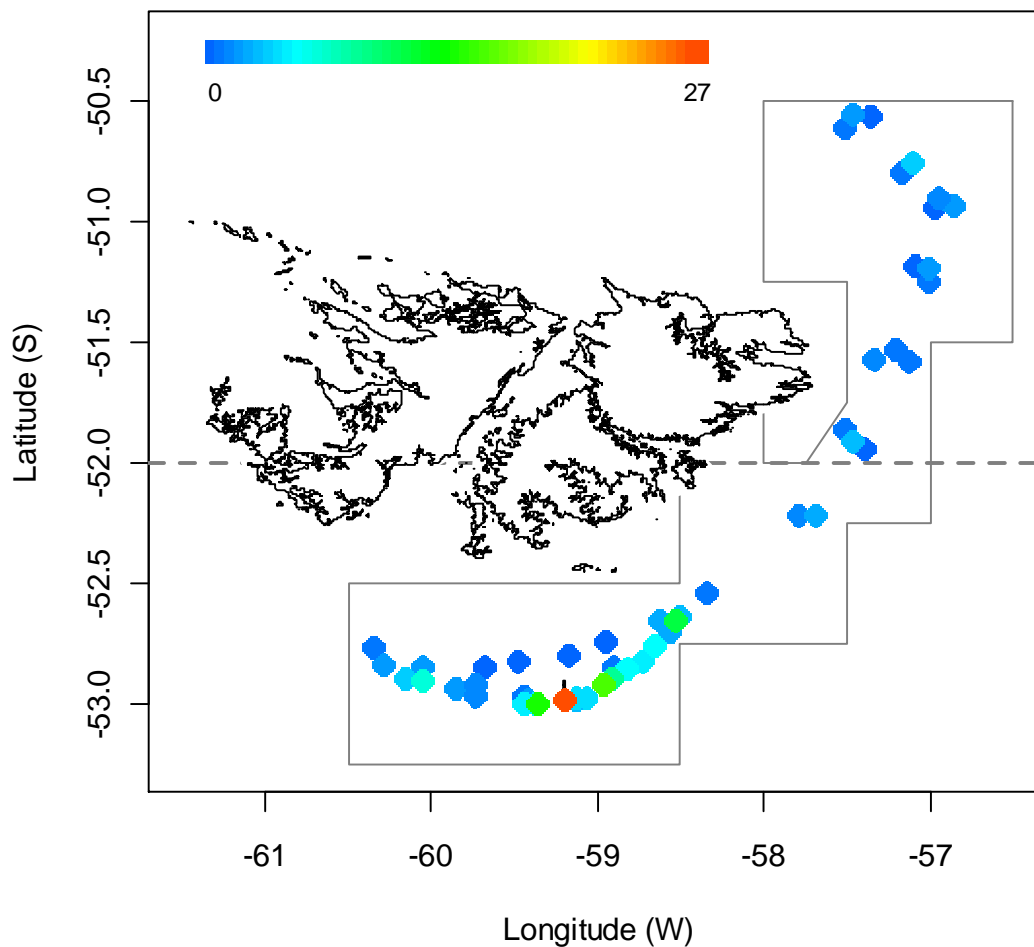
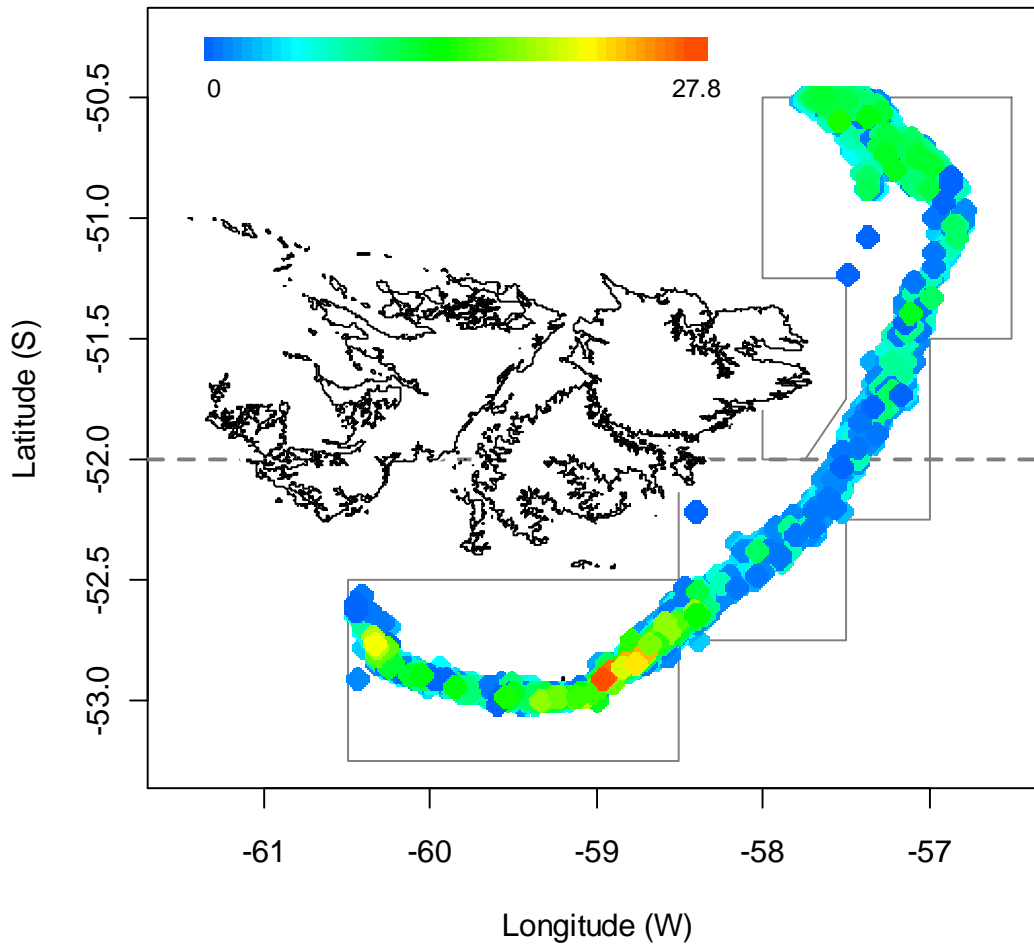


Figure 1. Spatial distribution of *Loligo* 2nd-season pre-season survey catches, colour-scaled to catch weight (maximum = 27.0 tonnes). Fifty-four catches are represented. The ‘Loligo Box’ fishing zone, as well as the 52 °S parallel delineating the boundary between north and south assessment sub-areas, are shown in gray.

Figure 2 [next page]. Spatial distribution of *Loligo* 2nd-season commercial catches, colour-scaled to catch weight (maximum = 27.8 tonnes). 4109 catches were taken during the season. The ‘Loligo Box’ fishing zone, as well as the 52 °S parallel delineating the boundary between north and south assessment sub-areas, are shown in gray.

Commercial, 15/07 - 30/09 2013



Methods

The depletion model formulated for the Falkland Islands *D. gahi* stock is based on the equivalence:

$$C_{\text{day}} = q \times E_{\text{day}} \times N_{\text{day}} \times e^{-M/2} \quad (1)$$

where q is the catchability coefficient, M is natural mortality (considered constant at 0.0133 day^{-1} ; Roa-Ureta and Arkhipkin, 2007), and C_{day} , E_{day} , N_{day} are catch (numbers of *D. gahi*), fishing effort (numbers of vessels), and abundance (numbers of *D. gahi*) per day. In its basic form (DeLury, 1947) the depletion model assumes a closed population in a fixed area for the duration of the assessment. However, the assumption of a closed population is imperfectly met in the Falkland Islands fishery, where stock analyses have often shown that *D. gahi* groups arrive in successive waves after the start of the season (Roa-Ureta, 2012; Winter and Arkhipkin, 2012). Arrivals of successive groups are inferred from discontinuities in the catch data. Fishing on a single, closed cohort would be expected to yield gradually decreasing CPUE, but gradually increasing average individual sizes, as the squid grow. When instead these

data change suddenly, or in contrast to expectation, the immigration of a new group to the population is indicated.

In the event of a new group arrival, the depletion calculation must be modified to account for this influx. This was done using a simultaneous algorithm (Roa-Ureta, 2012) that adds new arrivals on top of the stock previously present, and posits a common catchability coefficient for the entire depletion time-series. If two depletions are included in the same model (i.e., the stock present from the start plus a new group arrival), then:

$$C_{\text{day}} = q \times E_{\text{day}} \times (N1_{\text{day}} + (N2_{\text{day}} \times i2_{|0}^1)) \times e^{-M/2} \quad (2)$$

where $i2$ is a dummy variable taking the values 0 or 1 if 'day' is before or after the start day of the second depletion. For more than two depletions, $N3_{\text{day}}$, $i3$, $N4_{\text{day}}$, $i4$, etc., would be included following the same pattern.

The *D. gahi* stock assessment was calculated in a Bayesian framework (Punt and Hilborn, 1997), whereby results of the season depletion model are conditioned by prior information on the stock; in this case the information from the pre-season survey. The season depletion likelihood function was calculated as the difference between actual catch numbers reported and catch numbers predicted from the model, statistically corrected by a factor relating to the number of days of the depletion period (Roa-Ureta, 2012):

$$\left((n\text{Days} - 2) / 2 \right) \times \log \left(\sum_{\text{days}} \left(\log(\text{predicted } C_{\text{day}}) - \log(\text{actual } C_{\text{day}}) \right)^2 \right) \quad (3)$$

The survey prior likelihood function was calculated as the normal distribution of the difference between catchability (q) derived from the survey abundance estimate, and catchability derived from the season depletion model:

$$\frac{1}{\sqrt{2\pi \cdot SD_{q \text{ survey}}^2}} \times \exp \left(-\frac{(q_{\text{model}} - q_{\text{survey}})^2}{2 \cdot SD_{q \text{ survey}}^2} \right) \quad (4)$$

Catchability, rather than abundance N , was used for calculating the survey prior likelihood because catchability informs the entire season time series; whereas N from the survey only informs the first season depletion period – subsequent immigrations and depletions are independent of the abundance that was present during the survey.

Bayesian optimization of the model was then calculated by jointly minimizing equations (3) and (4). For joint minimization the prior and depletion functions were respectively weighted by the inverse of their coefficients of variation (CV), calculated as described in Appendices A and B. Distributions of the stock likelihood estimates (i.e., measures of their statistical uncertainty) were computed using a Markov Chain Monte Carlo (MCMC) (Gelman and Lopes, 2006), a method that is commonly employed for fisheries assessments (Magnusson et al., 2013). MCMC is an iterative process which generates random stepwise changes to the proposed outcome of a model (in this case, the N and q of *D. gahi*) and at each step, accepts or nullifies the change with a probability equivalent to how well the change fits the model parameters compared to the previous step. The resulting sequence of accepted or nullified

changes (i.e., the ‘chain’) approximates the likelihood distribution of the model outcome. The MCMC of the depletion models were run for 100,000 iterations; the first 1000 iterations were discarded as burn-in sections (initial phases over which the algorithm stabilizes); and the chains were thinned by a factor equivalent to the maximum of either 5 or the inverse of the acceptance rate (e.g., if the acceptance rate was 12.5%, then every 8th (0.125⁻¹) iteration was retained) to reduce serial correlation. For each model three chains were run; one chain initiated with the parameter values obtained from the joint optimization of equations (3) and (4), one chain initiated with these parameters $\times 2$, and one chain initiated with these parameters $\times 1/4$. Convergence of the three chains was accepted if the variance among chains was less than 10% higher than the variance within chains (Brooks and Gelman, 1998). When convergence was satisfied the three chains were combined as one set.

The estimate of *D. gahi* numbers on the final day of a time series is calculated as the numbers N of the depletion start days discounted for natural mortality during the intervening period, and subtracting cumulative catch also discounted for natural mortality (CNMD). Taking for example a two-depletion period:

$$N_{\text{final day}} = N1_{\text{start day 1}} \times e^{-M(\text{final day} - \text{start day 1})} + N2_{\text{start day 2}} \times e^{-M(\text{final day} - \text{start day 2})} - \text{CNMD}_{\text{final day}} \quad (5)$$

$$\text{CNMD}_{\text{day 1}} = 0$$

$$\text{CNMD}_{\text{day x}} = \text{CNMD}_{\text{day x-1}} \times e^{-M} + C_{\text{day x-1}} \times e^{-M/2}$$

$N_{\text{final day}}$ is then multiplied by the expected individual weight of *D. gahi* on the final day to give biomass. Expected individual weight is calculated using generalized additive models (GAM) applied to the time series of daily average individual sizes converted by the allometric length-weight relationship $W = \alpha \cdot L^\beta$ (Froese, 2006). Daily average individual sizes are obtained from mantle lengths measured in-season by observers, and also derived from in-season commercial data as the proportion of product weight that vessels reported per market size category. Observer mantle lengths are scientifically precise, but restricted to 1-2 vessels at any one time that may or may not be representative of the entire fleet. Commercially proportioned mantle lengths are relatively imprecise, but cover the entire fishing fleet every day. Therefore, both sources of data were used. Daily average individual weights were calculated by averaging observer size samples and commercial size categories where observer data were available, otherwise only commercial size categories.

The likelihood distribution of final day biomass was computed by drawing random normal values with mean and standard deviation from the GAM calculation for individual biomass on the final day, multiplying these values by random draws of $N_{\text{final day}}$ from equation (5) applied to the N_{start} outputs of the MCMC, and iterating the process 6 \times the number of MCMC outputs. Maximum likelihood of final day biomass was defined as the peak of the likelihood histogram with 1000-t intervals.

Stock assessment

Data

Commercial catches during the 2nd *Loligo* season showed a similar pattern to the 2nd pre-season survey (Winter et al., 2013), with highest concentrations near Beauchêne

Island (Figures 1 and 2). However, the commercial season also showed a second concentration of moderately high catches at the north end of the Loligo Box (Figure 2). Smaller catches were taken around the centre of the Loligo Box. Given this segregation, sub-areas north and south of 52° S were depletion-modelled separately.

Compared to previous 2nd seasons, daily catch totals taken during 2nd season of 2013 were relatively low. This was attributed to the frequently rough weather during the season (Figures 3 and 4) which inhibited effective fishing and dispersed the squid. It was noted that 41 X-licence daily catch reports submitted during the season listed a primary catch other than *Loligo*: 30 blue whiting, 7 red cod, 2 hoki, and 2 rock cod. Of these 41 reports, the primary catch was ≥ 10 t in all except 4, and ≥ 20 t in all except 14. It was also noted that between the beginning of *Loligo* season (July 15) and the end of October, 39 finfish-licence daily catch reports and 1 skate-licence daily catch report listed *Loligo* catch ≥ 1 t, of which 7 ≥ 2 t, and 3 ≥ 5 t. The three catch reports with ≥ 5 t *Loligo* were all west of 60° W (grids XJAG, XPAD and XVAD), further suggesting a wide dispersal of *D. gahi* in this season.

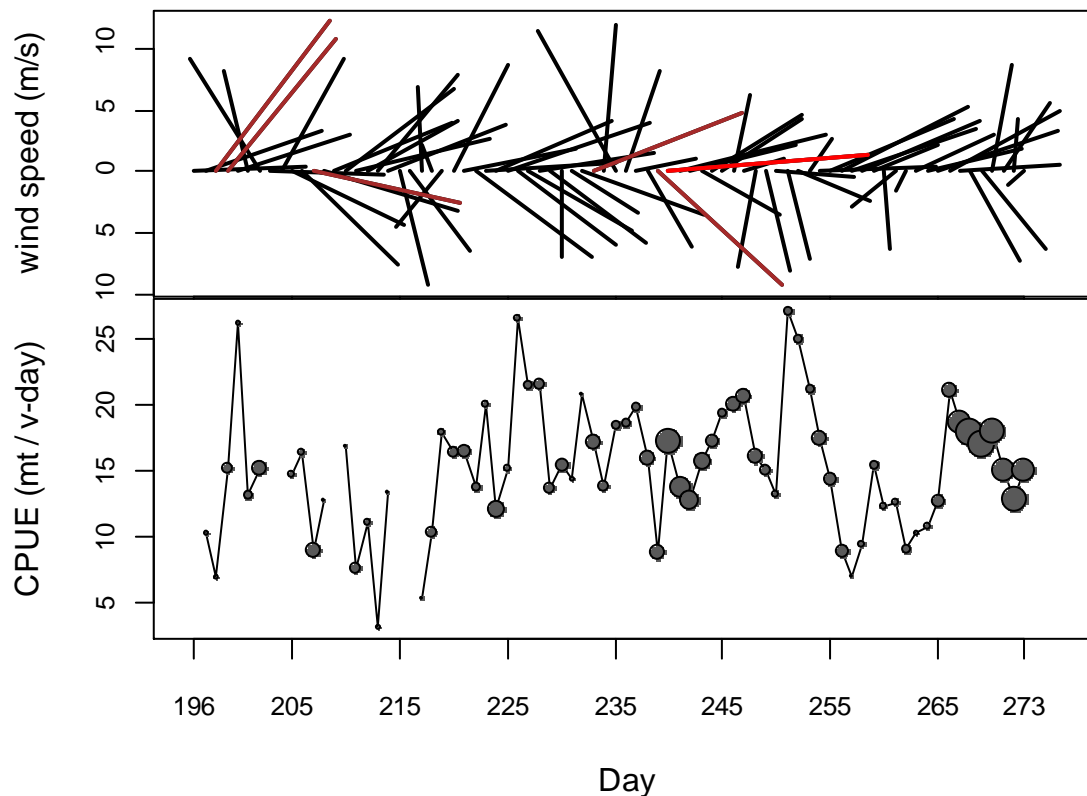
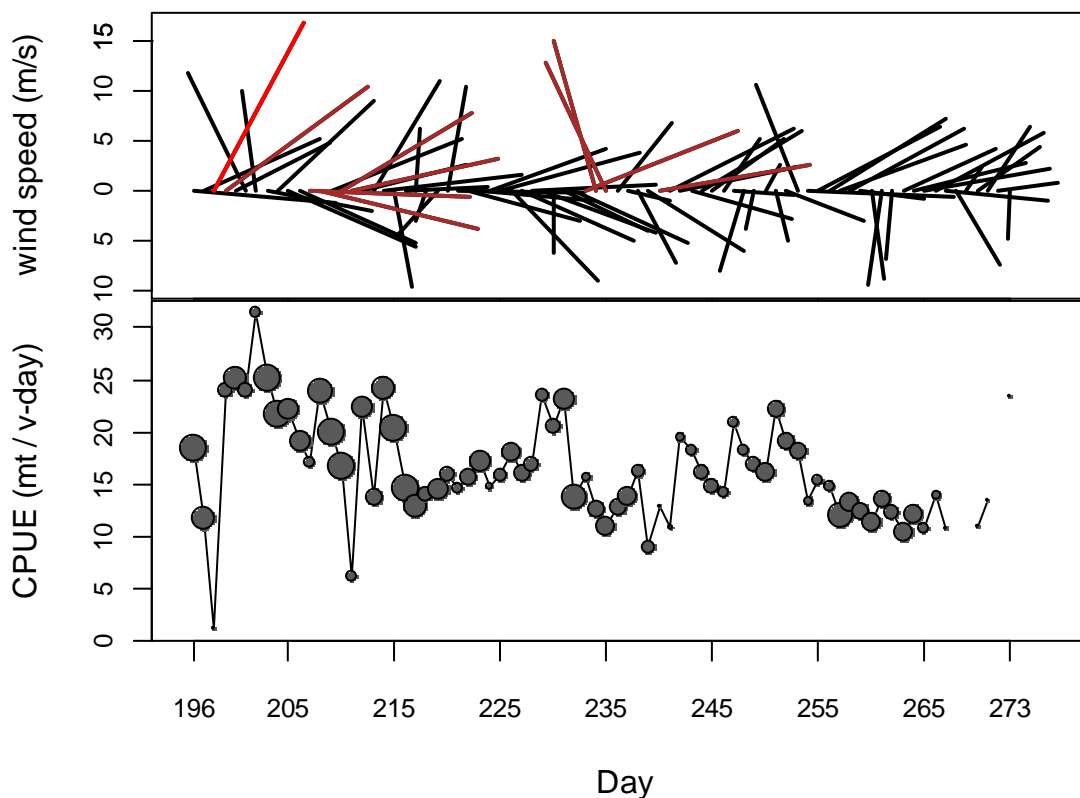


Figure 3. Top: average wind vectors (from NCDC-NOAA; Zhang et al., 2006) per day at the north sub-area fishing midpoint. Brown vectors: high wind (Beaufort wind force scale 7; ≥ 13.9 m/s). Red vectors: gale (Beaufort wind force scale 8; ≥ 17.2 m/s). Bottom: CPUE in the north sub-area on corresponding days (equivalent to Figure 7).

Figure 4 [next page]. Top: average wind vectors (from NCDC-NOAA; Zhang et al., 2006) per day at the south sub-area fishing midpoint. Brown vectors: high wind (Beaufort wind force scale 7; ≥ 13.9 m/s). Red vectors: gale (Beaufort wind force scale 8; ≥ 17.2 m/s). Bottom: CPUE in the south sub-area on corresponding days (equivalent to Figure 7).



Between 5 and 16 vessels fished in the commercial season on any day (median = 16; Figure 5), for a total of 1195 vessel-days. These vessels reported daily catch totals to the FIFD and electronic logbook data that included trawl times, positions, and product weight by market size categories.

Two FIFD observers were deployed on three vessels in the fishery for a total of 95 observer-days. Throughout the 78 days of the season, 2 days had no observer covering, 57 days had 1 observer covering, and 19 days had two observers covering. Observers sampled an average of 411 *D. gahi* daily, and reported their maturity stages, sex, and lengths to 0.5 cm. The length-weight relationship for converting both observer and commercially proportioned length data was taken from the pre-season survey (Winter et al., 2013):

$$\text{weight (kg)} = 0.109 \times \text{length (cm)}^{2.373} / 1000 \quad (6)$$

Group arrivals / depletion criteria

Start and end days of depletions - following arrivals of new *D. gahi* groups - were judged primarily with reference to daily changes in CPUE, with additional information from sex proportions, maturity, and average individual *D. gahi* sizes. CPUE was calculated as metric tonnes of *D. gahi* caught per vessel per day. Days were used rather than trawl hours as the basic unit of effort. Commercial vessels do not trawl standardized duration hours, but rather durations that best suit their daily processing requirements. An effort index of days is therefore more consistent.

Four days in the north and three days in the south were identified that most plausibly represented the onset of separate depletions.

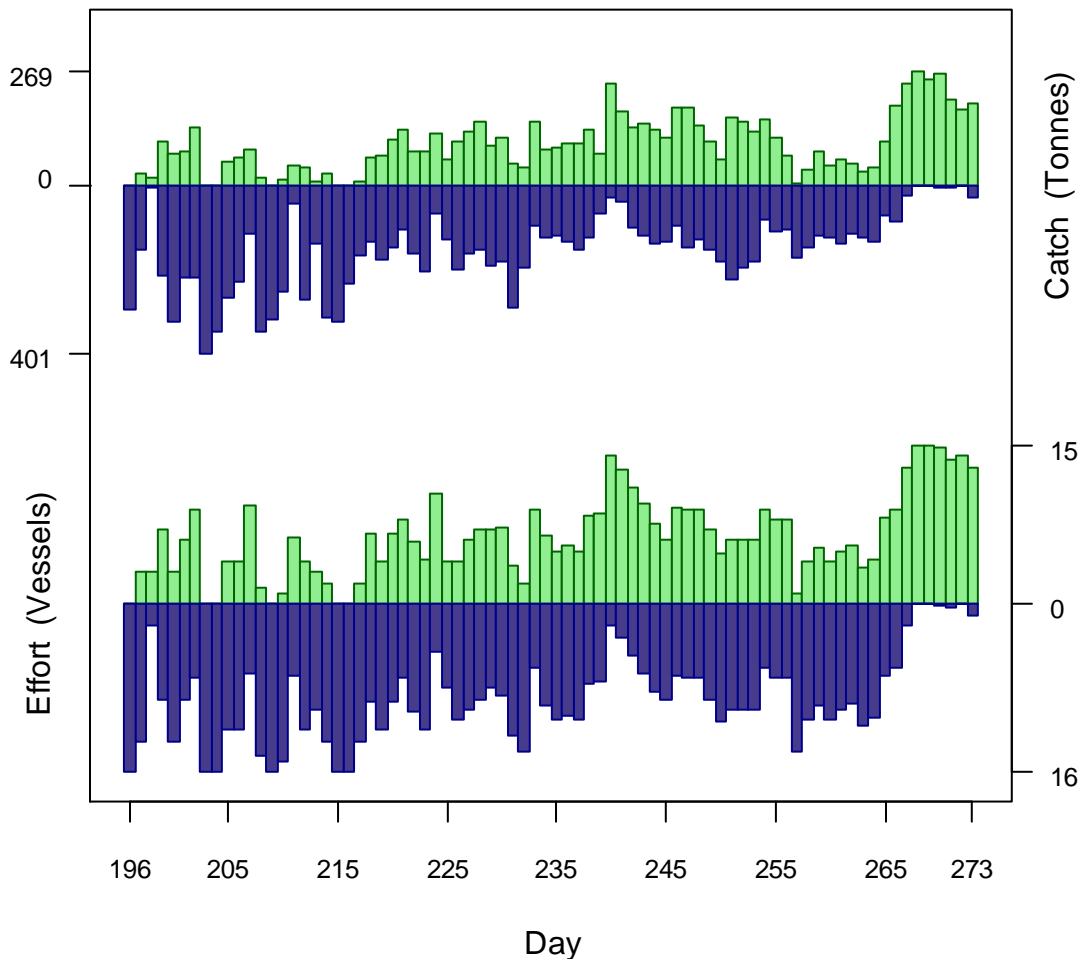


Figure 5. Daily total *D. gahi* catch and effort distribution by assessment sub-area north (green) and south (purple) of the 52° S parallel in the *Loligo* 2nd season 2013. The season was open from July 15th (chronological day 196) to September 30th (chronological day 273). As many as 15 vessels fished per day north of 52° S; as many as 16 vessels fished per day south of 52° S. As much as 269 tonnes *D. gahi* was caught per day north of 52° S; as much as 401 tonnes *D. gahi* was caught per day south of 52° S.

- The first in-season depletion north was identified on day 200 (19th July), with a peak in average commercial weight (Figure 6), and a strong increase in CPUE over 2 days (Figure 7).
- The second and third in-season depletions north were identified on day 226 (14th August) and day 251 (8th September) with strong CPUE peaks (Figure 7).
- The fourth in-season depletion north was identified on day 266 (23rd September) with an increase in CPUE followed by 4 days of CPUE that were higher than any CPUE for 10 days before (Figure 7). Day 266 also represented a peak in the proportion of female *D. gahi*, as sampled by the observer (Figure 6).
- The first in-season depletion south was identified on day 202 (21st July) with the highest CPUE peak of the season (Figure 7).
- The second in-season depletion south was identified on day 229 (17th August) with a moderate CPUE increase (Figure 7).
- The third in-season depletion south was identified on day 251 (8th September) with a moderate CPUE peak, followed by a continuous period of CPUE decrease to the end of the season (Figure 7).

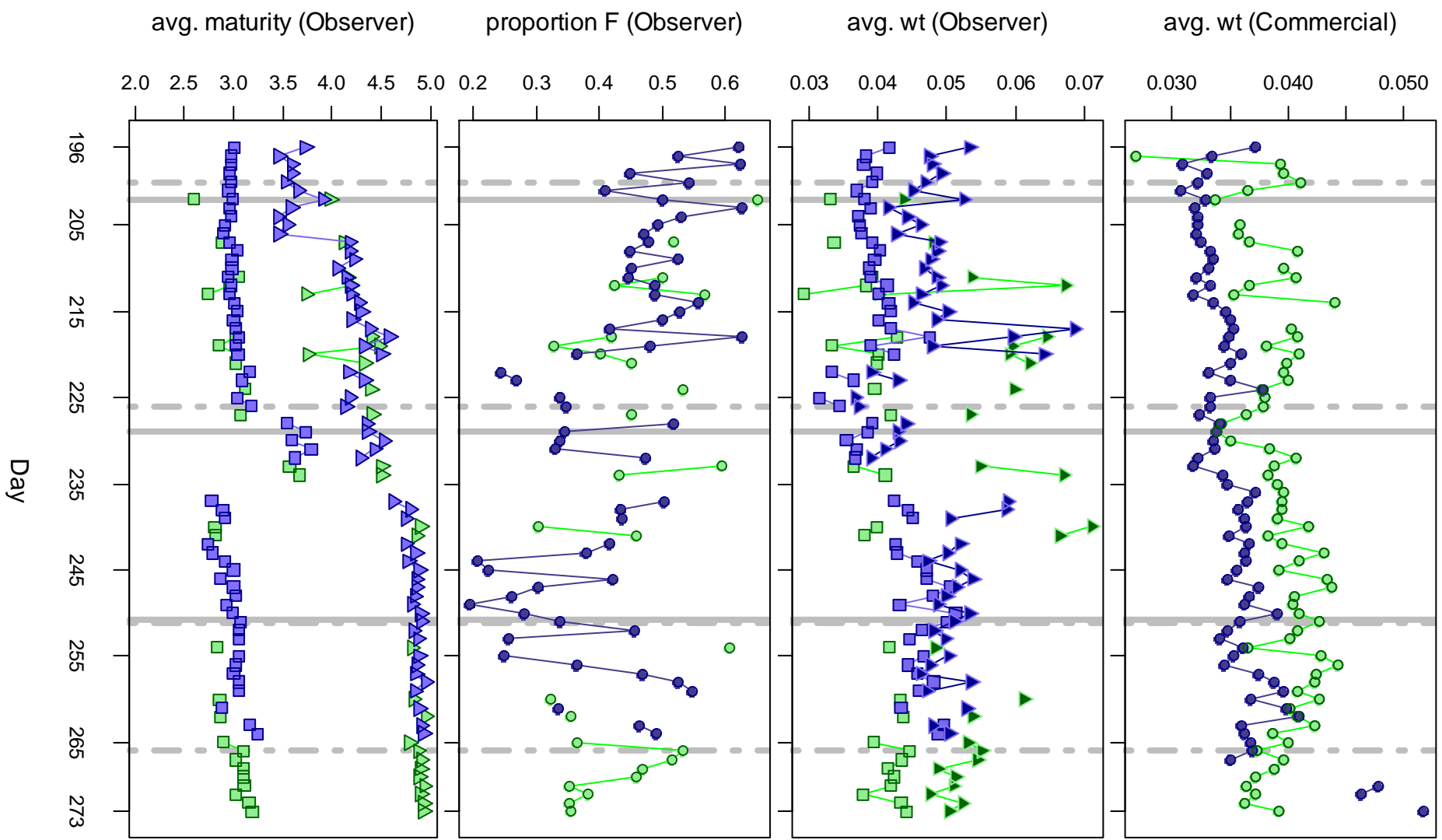


Figure 6 [Previous page]. Top graph: Average individual *D. gahi* weights (kg) per day from commercial size categories. 2nd graph: Average individual *D. gahi* weights (kg) by sex per day from observer sampling. 3rd graph: Proportions of female *D. gahi* per day from observer sampling. Bottom graph: avg. maturity value by sex per day from observer sampling. Males: triangles, females: squares, unsexed: circles. North sub-area: green, south sub-area: purple. Data from consecutive days are joined by line segments. Broken gray bars indicate days 200, 226, 251 and 266, identified as the start of in-season depletion or immigration north. Solid gray bars indicate days 202, 229, and 251, identified as the start of in-season depletion south.

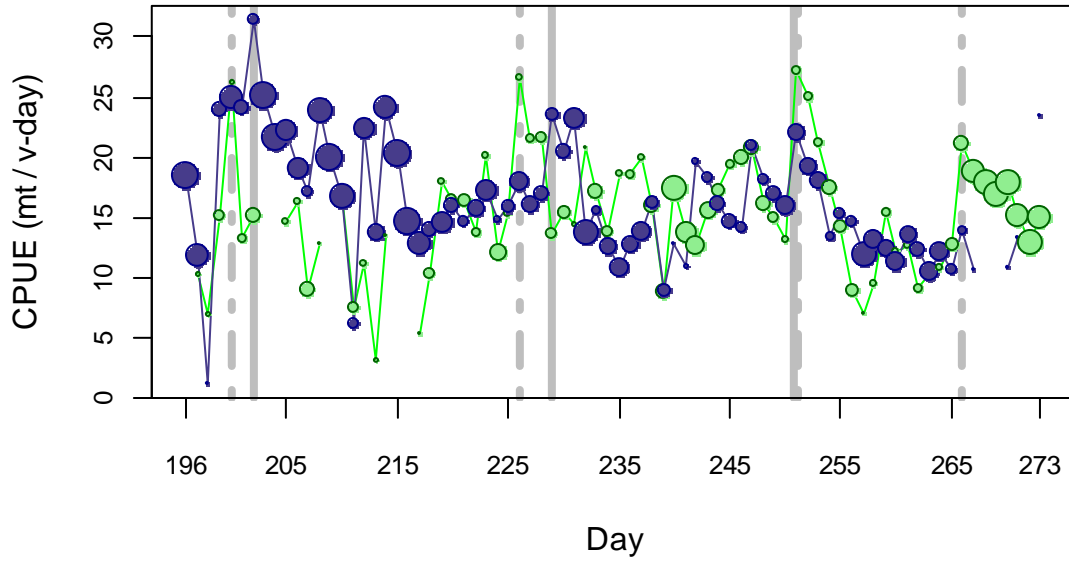


Figure 7. CPUE in metric tonnes per vessel per day, by assessment sub-area north (green) and south (purple) of the 52° S parallel. Circle sizes are proportioned to the numbers of vessels fishing. Data from consecutive days are joined by line segments. Broken gray bars indicate days 200, 226, 251 and 266, identified as the start of in-season depletion or immigration north. Solid gray bars indicate days 202, 229, and 251, identified as the start of in-season depletion south.

Depletion analyses

South

In the south sub-area, MCMC revealed that the Bayesian model stabilized in two alternate states: low catchability coefficient q with corresponding high N values, and high catchability q with low N (Appendix C, Figure A3). The low q state corresponded to N values in excess of 2.5 billion *D. gahi* for the first immigration peak alone, which was unrealistic and considered a spurious optimization. Parameter iterations corresponding to $q \leq 0.00035$ (see horizontal line through the top graph of Figure A3) were therefore excluded from calculating the likelihood distribution of the south sub-area abundance.

With this constraint, Bayesian optimization on catchability (q) showed an intermediate posterior outcome (max. likelihood $q_S = 0.625 \times 10^{-3}$; Figure 8, left); lower than the pre-season survey (prior $q_S = 1.389 \times 10^{-3}$; Appendix A), and higher than the in-season depletion (depletion $q_S = 0.353 \times 10^{-3}$; Appendix B).

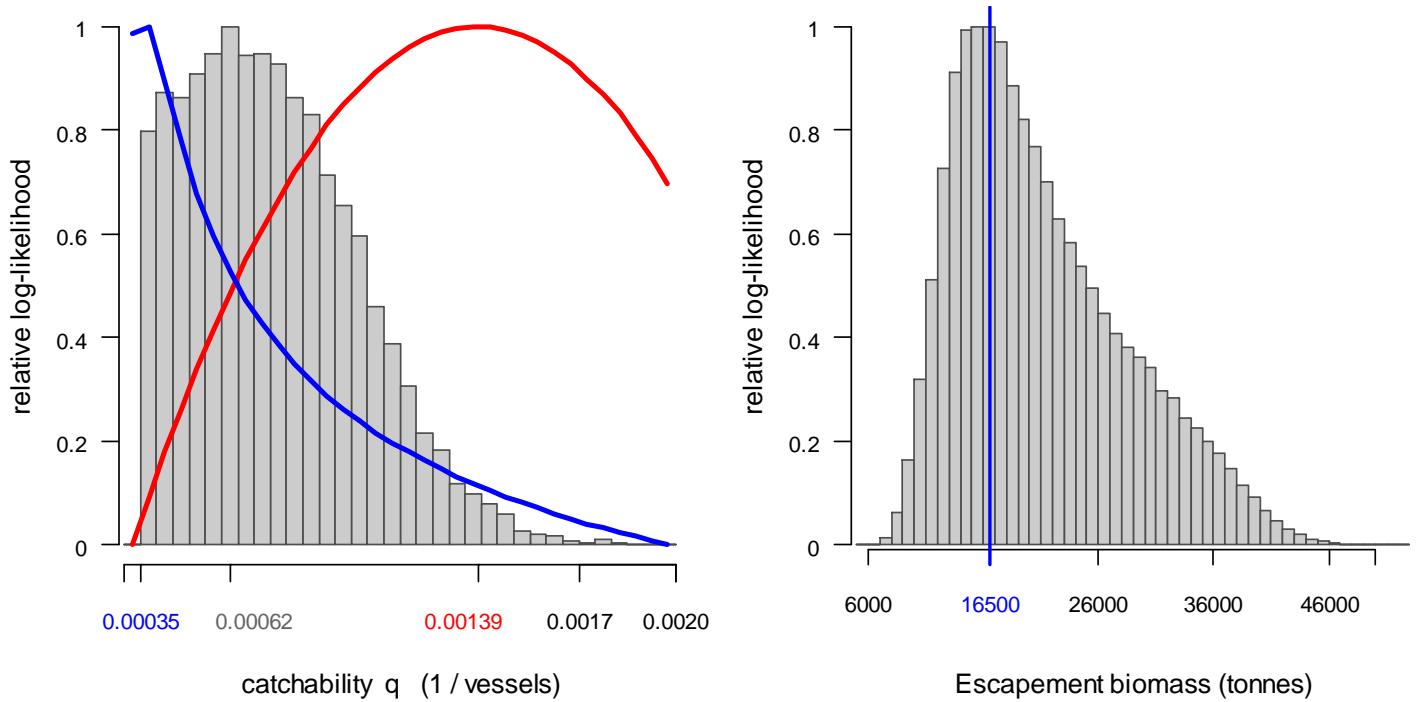


Figure 8. North sub-area. Left: Likelihood distributions for *D. gahi* catchability. Red line: prior model (pre-season survey data), blue line: in-season depletion model, gray bars: combined Bayesian model. Right: Likelihood distribution of escapement biomass, from Bayesian posterior and expected average individual *D. gahi* weight at the end of the season.

The MCMC distribution of the posterior outcome, together with the GAM distribution of average individual *D. gahi* weight on the final day of the season (49.0 ± 2.5 g; Appendix D, Figure A4, bottom), gave the likelihood distribution of *D. gahi* final-day biomass shown in Figure 8, right, with maximum likelihood and 95% confidence interval of:

$$B_{S \text{ day } 273} = 16,500 \text{ t} \sim 95\% \text{ CI } [10,579 - 37,919] \text{ t} \quad (7)$$

North

In the north sub-area, Bayesian optimization on catchability (q) showed a stronger effect of the pre-season survey ($q_{\text{prior}} = 1.932 \times 10^{-3}$; Appendix A) than of in-season depletion ($q_{\text{depletion}} = 0.506 \times 10^{-3}$; Appendix B) on the posterior outcome (max. likelihood $q_N = 1.825 \times 10^{-3}$; Figure 9, left).

The MCMC distribution of the posterior outcome, together with the GAM distribution of average individual *D. gahi* weight on the final day of the season (43.3 ± 1.0 g; Appendix D, Figure A4, top), gave the likelihood distribution of *D. gahi* final-day biomass shown in Figure 9, right, with maximum likelihood and 95% confidence interval of:

$$B_{N \text{ day } 273} = 8,500 \text{ t} \sim 95\% \text{ CI } [5,896 - 15,113] \text{ t} \quad (8)$$

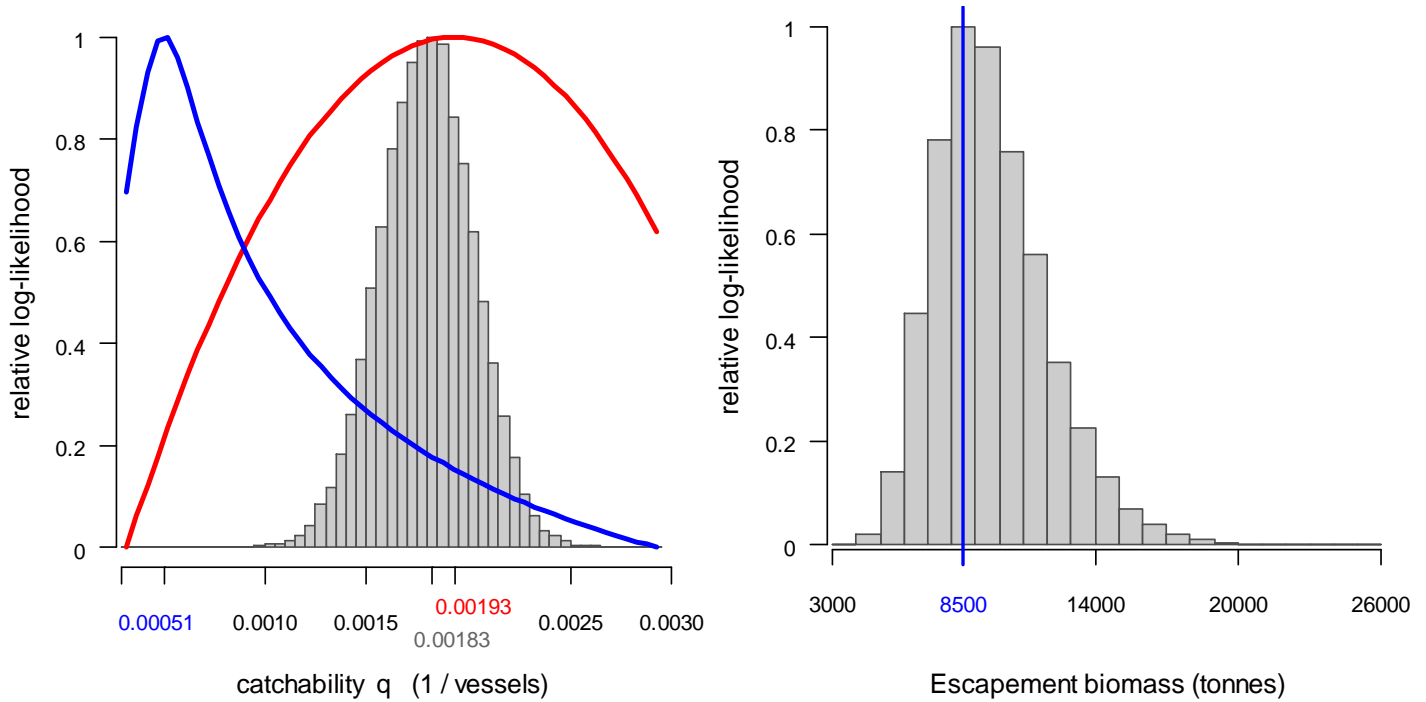


Figure 9. North sub-area. Left: Likelihood distributions for *D. gahi* catchability. Red line: prior model (pre-season survey data), blue line: in-season depletion model, gray bars: combined Bayesian model. Right: Likelihood distribution of escapement biomass, from Bayesian posterior and expected average individual *D. gahi* weight at the end of the season.

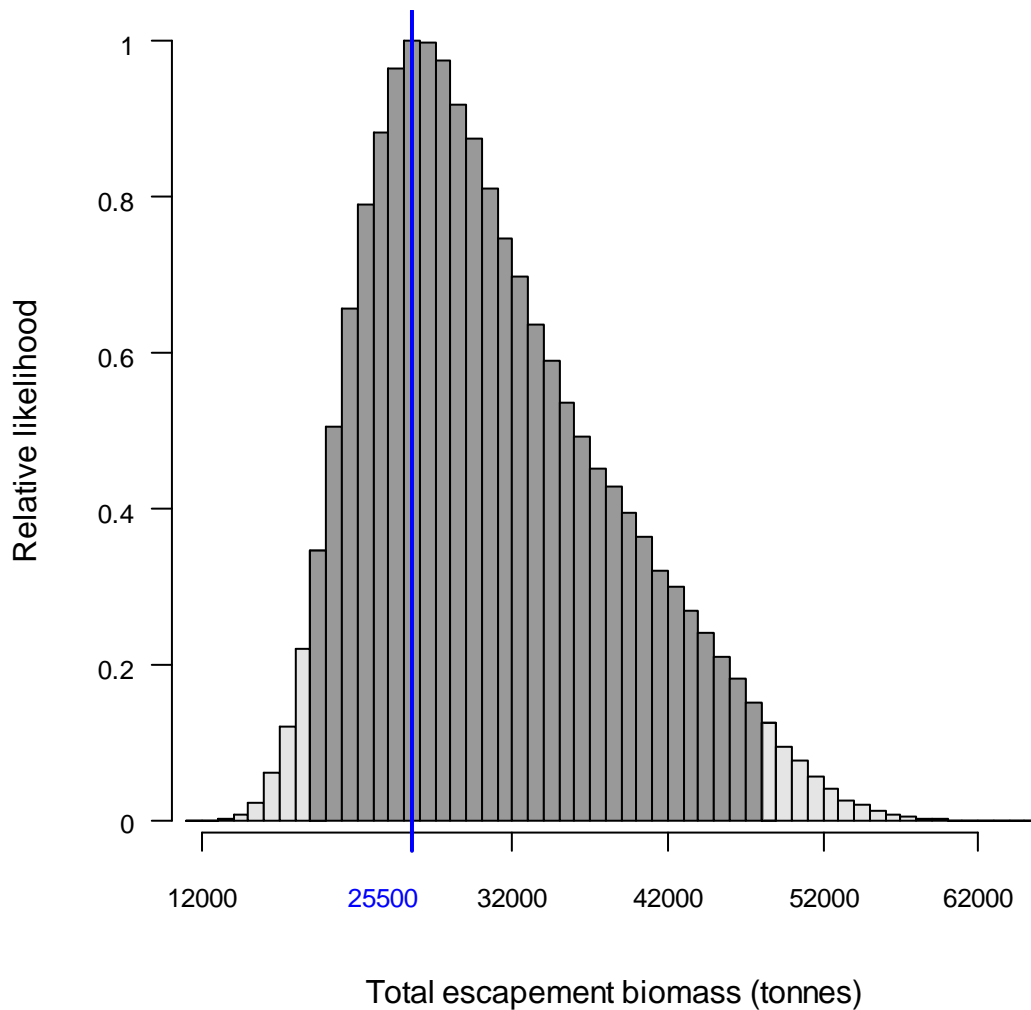
Escapement biomass

Escapement biomass was defined as the aggregate biomass of *D. gahi* at the end of the season (day 273; September 30th) for the north and south sub-areas combined (equations (7) plus (8)). The north and south sub-area biomasses are assumed to be independent and therefore the aggregate was calculated by adding the respective north and south likelihood distributions in random order. The likelihood distribution of the aggregate escapement biomass is shown in Figure 10. Asymmetry of the respective north and south distributions (Figures 8-right and 9-right) results in the maximum likelihood of the aggregate distribution being non-identical to the sum of maximum likelihoods of the separate north and south distributions.

$$\begin{aligned}
 B_{\text{Total day 107}} &= B_{\text{N day 273}} + B_{\text{S day 273}} \\
 &= 25,500 \text{ t} \sim 95\% \text{ CI } [19,014 - 48,197] \text{ t} \quad (9)
 \end{aligned}$$

The risk of the fishery, defined as the proportion of the escapement biomass distribution below the conservation limit of 10,000 tonnes (Agnew et al., 2002; Barton, 2002), was calculated as effectively zero.

Figure 10 [next page]. Likelihood distribution of *D. gahi* escapement biomass at the end of the season, September 30th. The 95% interval of the distribution is shaded darker gray.



Immigration

D. gahi immigration during the season was inferred as the difference between *D. gahi* biomass at the end of the pre-season survey (Winter et al., 2013) and *D. gahi* biomass at the end of the commercial season (escapement biomass) plus catch. The likelihood distribution of this difference was calculated by repeated iterations of drawing a random value from the escapement biomass distribution (equation (9)), adding the season catch, and subtracting a random draw from the likelihood distribution of the pre-season survey biomass:

$$\begin{aligned}
 B_{\text{Season Immigration}} &= B_{\text{Total day 273}} + C_{\text{Season}} - B_{\text{Survey end}} \\
 &= 25,500 [19,014 - 48,197] + 19,614 \\
 &\quad - 36,283 [31,359 - 41,162] \\
 &= 9,500 \text{ t} \sim 95\% \text{ CI } [1,041 - 32,173] \text{ t}
 \end{aligned}
 \tag{10}$$

Note that this represents, more specifically, the biomass resulting from immigration rather than the biomass that immigrated; it is not taken into account that the squid would have been smaller on the date they entered the fishing zone and subsequently grown. However, in-season natural mortality is taken into account through the CNMD

factor (equation (5)). By this estimate, in-season immigration represents 21% of the *D. gahi* biomass to have been present in the fishing zone in the 2nd season of 2013: $9,500/(25,500 + 19,614) = 0.211$.

References

- Agnew, D.J., Baranowski, R., Beddington, J.R., des Clers, S., Nolan, C.P. 1998. Approaches to assessing stocks of *Loligo gahi* around the Falkland Islands. *Fisheries Research* 35:155-169.
- Agnew, D. J., Beddington, J. R., and Hill, S. 2002. The potential use of environmental information to manage squid stocks. *Canadian Journal of Fisheries and Aquatic Sciences*, 59: 1851–1857.
- Arkhipkin, A.I., Middleton, D.A.J., Barton, J. 2008. Management and conservation of a short-lived fishery resource: *Loligo gahi* around the Falkland Islands. *American Fisheries Society Symposium* 49:1243-1252.
- Barton, J. 2002. Fisheries and fisheries management in Falkland Islands Conservation Zones. *Aquatic Conservation: Marine and Freshwater Ecosystems*, 12: 127–135.
- Brooks, S.P., Gelman, A. 1998. General methods for monitoring convergence of iterative simulations. *Journal of computational and graphical statistics* 7:434-455.
- DeLury, D.B. 1947. On the estimation of biological populations. *Biometrics* 3:145-167.
- Froese, R. 2006. Cube law, condition factor and weight–length relationships: history, meta-analysis and recommendations. *Journal of Applied Ichthyology*, 22: 241–253.
- Gamerman, D., Lopes, H.F. 2006. Markov Chain Monte Carlo. Stochastic simulation for Bayesian inference. 2nd edition. Chapman & Hall/CRC.
- Magnusson, A., Punt, A., Hilborn, R. 2013. Measuring uncertainty in fisheries stock assessment: the delta method, bootstrap, and MCMC. *Fish and Fisheries* 14: 325-342.
- Patterson, K.R. 1988. Life history of Patagonian squid *Loligo gahi* and growth parameter estimates using least-squares fits to linear and von Bertalanffy models. *Marine Ecology Progress Series* 47:65-74.
- Payá, I. 2010. Fishery Report. *Loligo gahi*, Second Season 2009. Fishery statistics, biological trends, stock assessment and risk analysis. Technical Document, Falkland Islands Fisheries Department.
- Punt, A.E., Hilborn, R. 1997. Fisheries stock assessment and decision analysis: the Bayesian approach. *Reviews in Fish Biology and Fisheries* 7:35-63.
- Roa-Ureta, R. 2012. Modelling in-season pulses of recruitment and hyperstability-hyperdepletion in the *Loligo gahi* fishery around the Falkland Islands with generalized depletion models. *ICES Journal of Marine Science*, 69: 1403–1415.
- Roa-Ureta, R., Arkhipkin, A.I. 2007. Short-term stock assessment of *Loligo gahi* at the Falkland Islands: sequential use of stochastic biomass projection and stock depletion models. *ICES Journal of Marine Science* 64:3-17.

- Rosenberg, A.A., Kirkwood, G.P., Crombie, J.A., Beddington, J.R. 1990. The assessment of stocks of annual squid species. *Fisheries Research* 8:335-350.
- Winter, A., Arkhipkin, A. 2012. Predicting recruitment pulses of Patagonian squid in the Falkland Islands fishery. World Fisheries Congress, Edinburgh, Scotland.
- Winter, A., Blake, A., Sobrado, F. 2013. *Loligo* stock assessment survey, 2nd season 2013. Technical Document, Falkland Islands Fisheries Department.
- Zhang, H.-M., Bates, J.J., Reynolds, R.W. 2006. Assessment of composite global sampling: Sea surface wind speed. *Geophysical Research Letters*, 33: L17714.

Appendix

A. Prior estimates and CV

The pre-season survey (Winter et al., 2013) had estimated *D. gahi* biomasses of 11,740 t (standard deviation: $\pm 1,142$ t) north of 52° S and 24,544 t (standard deviation: $\pm 2,157$ t) south of 52° S. From acoustic data analyses, Payá (2010) estimated a net escapement of up to 22%, which was added to the standard deviation:

$$11,740 \pm \left(\frac{1,142}{11,740} + .22 \right) = 11,740 \pm 31.7\% = 11,740 \pm 3,724 \text{ t.} \quad (\text{A1-N})$$

$$24,544 \pm \left(\frac{2,157}{24,544} + .22 \right) = 24,544 \pm 30.8\% = 24,544 \pm 7,557 \text{ t.} \quad (\text{A1-S})$$

The 22% was added as a linear increase in the variability, but was not used to reduce the total estimate, because *D. gahi* that escape one trawl are likely to be part of the biomass concentration that is available to the next trawl. This estimate in biomass was converted to an estimate in numbers using the size-frequency distributions sampled during the pre-season survey (Winter et al., 2013).

D. gahi were sampled at 55 pre-season survey stations, giving average mantle lengths (both sexes; weighted for *D. gahi* density distribution) of 11.16 cm north and 11.70 cm south, corresponding to respectively 0.033 and 0.037 kg average individual weight. Error distributions of average individual weight were estimated by randomly re-sampling the length-frequency data 10,000×, giving coefficients of variation 0.80% north and 0.84% south. Average coefficients of variation of the length-weight relationship (equation (6)) were 7.95% north and 8.00% south. Combining all sources of variation with the pre-season survey biomass estimates and average individual weights gave estimated *D. gahi* numbers at season start (July 15th; day 196) of:

$$\begin{aligned} \text{prior } N_{N \text{ day } 196} &= \frac{11,740 \times 1000}{0.033} \pm \sqrt{31.7\%^2 + 0.80\%^2 + 7.95\%^2} \\ &= 0.353 \times 10^9 \pm 32.7\% = 0.353 \times 10^9 \pm 0.115 \times 10^9 \end{aligned} \quad (\text{A2-N})$$

$$\begin{aligned} \text{prior } N_{S \text{ day } 196} &= \frac{24,544 \times 1000}{0.037} \pm \sqrt{30.8\%^2 + 0.84\%^2 + 8.00\%^2} \\ &= 0.659 \times 10^9 \pm 31.8\% = 0.659 \times 10^9 \pm 0.210 \times 10^9 \end{aligned} \quad (\text{A2-S})$$

D. gahi numbers projected to the start of the depletion time series (day 200 north and day 202 south, e.g., Figures 6 and 7) were calculated according to equation (5):

$$\begin{aligned} \text{prior } N_{N \text{ day } 200} &= \text{prior } N_{N \text{ day } 196} \times e^{-M(200-196)} - \text{CNMD}_{N \text{ day } 200} \\ &= 0.353 \times 10^9 \times 0.948 - 0.004 \times 10^9 \\ &= 0.330 \times 10^9 \end{aligned} \quad (\text{A3-N})$$

$$\text{prior } N_{S \text{ day } 202} = \text{prior } N_{S \text{ day } 196} \times e^{-M(202-196)} - \text{CNMD}_{S \text{ day } 202}$$

$$\begin{aligned}
&= 0.659 \times 10^9 \times 0.923 - 0.030 \times 10^9 \\
&= 0.579 \times 10^9
\end{aligned}
\tag{A3-S}$$

Corresponding catchability coefficients (q) calculated at the start of depletion time series were then:

$$\begin{aligned}
\text{prior } q_N &= C(N)_{N \text{ day } 200} / (\text{prior } N_{N \text{ day } 200} \times E_{N \text{ day } 200}) \\
&= (C(B)_{N \text{ day } 200} / Wt_{N \text{ day } 200}) / (\text{prior } N_{N \text{ day } 200} \times E_{N \text{ day } 200}) \\
&= (78.7 \text{ t} / 0.041 \text{ kg}) / (0.330 \times 10^9 \times 3 \text{ vessel-days}) \\
&= 1.932 \times 10^{-3} \text{ vessels}^{-1}
\end{aligned}
\tag{A4-N}$$

$$\begin{aligned}
\text{prior } q_S &= C(N)_{S \text{ day } 202} / (\text{prior } N_{S \text{ day } 202} \times E_{S \text{ day } 202}) \\
&= (C(B)_{S \text{ day } 202} / Wt_{S \text{ day } 202}) / (\text{prior } N_{S \text{ day } 202} \times E_{S \text{ day } 202}) \\
&= (219.8 \text{ t} / 0.039 \text{ kg}) / (0.579 \times 10^9 \times 7 \text{ vessel-days}) \\
&= 1.389 \times 10^{-3} \text{ vessels}^{-1}
\end{aligned}
\tag{A4-S}$$

with error estimates (CV) equal to the sum of errors of the N calculations (equations A2) plus CVs of catch by vessels on those days:

$$\begin{aligned}
CV_{\text{prior } q_N} &= \sqrt{32.7\% ^2 + \left(\frac{SD(C(B)_{N \text{ vessels day } 200})}{\text{mean}(C(B)_{N \text{ vessels day } 200})} \right)^2} \\
&= \sqrt{32.7\% ^2 + 12.2\% ^2} = 34.9\%
\end{aligned}
\tag{A5-N}$$

$$\begin{aligned}
CV_{\text{prior } q_S} &= \sqrt{31.8\% ^2 + \left(\frac{SD(C(B)_{S \text{ vessels day } 202})}{\text{mean}(C(B)_{S \text{ vessels day } 202})} \right)^2} \\
&= \sqrt{31.8\% ^2 + 58.6\% ^2} = 66.7\%
\end{aligned}
\tag{A5-S}$$

B. Depletion model estimates and CV

For the north sub-area, the equivalent of equation (2) with four N_{day} was optimized on the difference between predicted catches and actual catches (equation (3)), resulting in parameters values:

$$\begin{aligned}
\text{depletion } N1_{N \text{ day } 200} &= 0.737 \times 10^9; & \text{depletion } N2_{N \text{ day } 226} &= 0.520 \times 10^9 \\
\text{depletion } N3_{N \text{ day } 251} &= 0.054 \times 10^9; & \text{depletion } N4_{N \text{ day } 266} &= 0.280 \times 10^9 \\
\text{depletion } q_N &= 0.506 \times 10^{-3} \text{ vessels}^{-1}
\end{aligned}$$

The root-mean-square deviation of predicted vs. actual catches was calculated, and its CV assigned to the depletion model q parameter:

$$\begin{aligned}
CV_{\text{depletion } q_N} &= \frac{\sqrt{\sum_i \left(\text{predicted } C(N)_{N \text{ day } i} - \text{actual } C(N)_{N \text{ day } i} \right)^2}}{\text{mean}(\text{actual } C(N)_{N \text{ day } i})} \\
&= 0.625 \times 10^6 / 2.463 \times 10^6 = 25.4\% \quad (\text{A6-N})
\end{aligned}$$

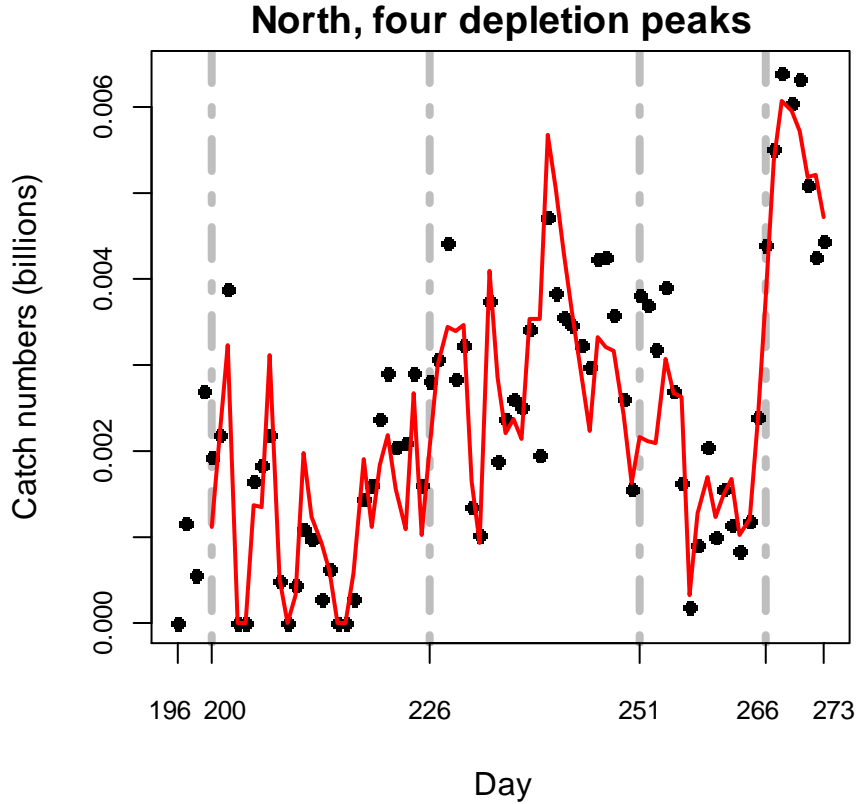


Figure A1. Daily catch numbers estimated from actual catch (black points) and predicted from the depletion model (red line) in the north sub-area.

For the south sub-area, the equivalent of equation (2) with three N_{day} was optimized on the difference between predicted catches and actual catches (equation (3)), resulting in parameters values:

$$\text{depletion } N1_{S \text{ day } 202} = 1.622 \times 10^9; \quad \text{depletion } N2_{S \text{ day } 229} = 0.340 \times 10^9$$

$$\text{depletion } N3_{S \text{ day } 251} = 0.187 \times 10^9$$

$$\text{depletion } q_S = 0.353 \times 10^{-3} \text{ vessels}^{-1}$$

The root-mean-square deviation of predicted vs. actual catches was calculated, and its CV assigned to the depletion model q parameter:

$$\begin{aligned}
CV_{\text{depletion } q_S} &= \frac{\sqrt{\sum_i \left(\text{predicted } C(N)_{S \text{ day } i} - \text{actual } C(N)_{S \text{ day } i} \right)^2}}{\text{mean}(\text{actual } C(N)_{S \text{ day } i})}
\end{aligned}$$

$$= 0.935 \times 10^6 / 4.142 \times 10^6 = 22.6\%$$

(A6-S)

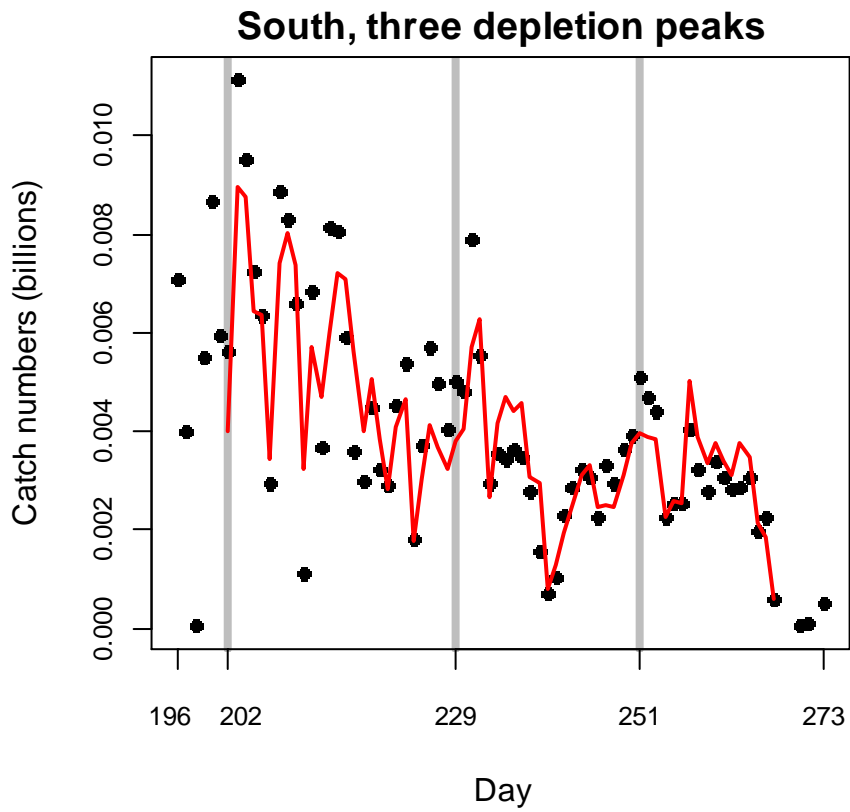
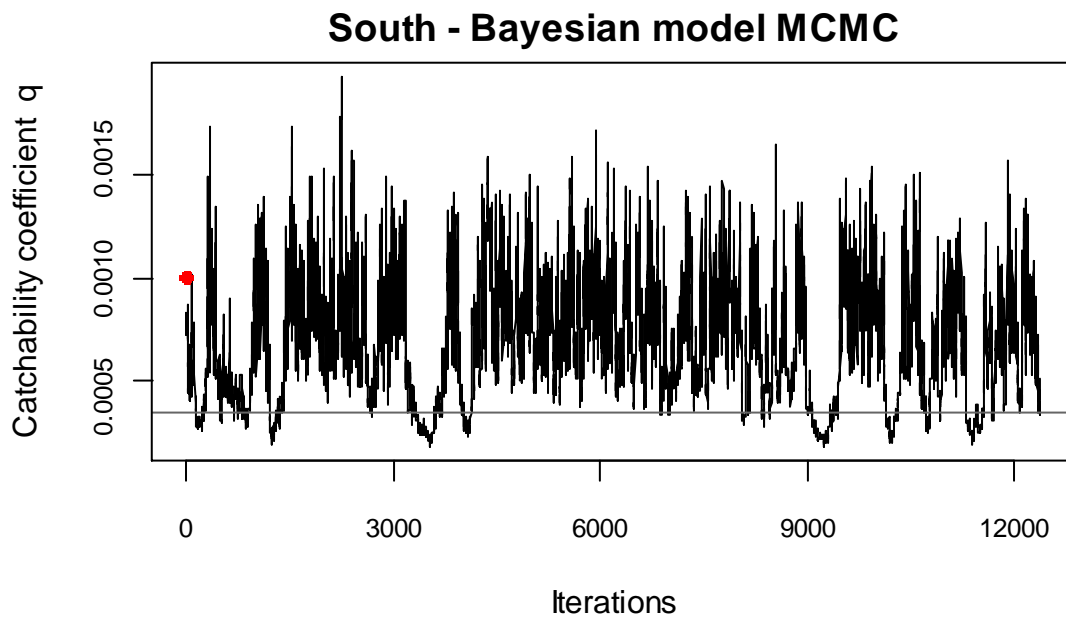


Figure A2. Daily catch numbers estimated from actual catch (black points) and predicted from the depletion model (red line) in the south sub-area.

C. MCMC restrictions



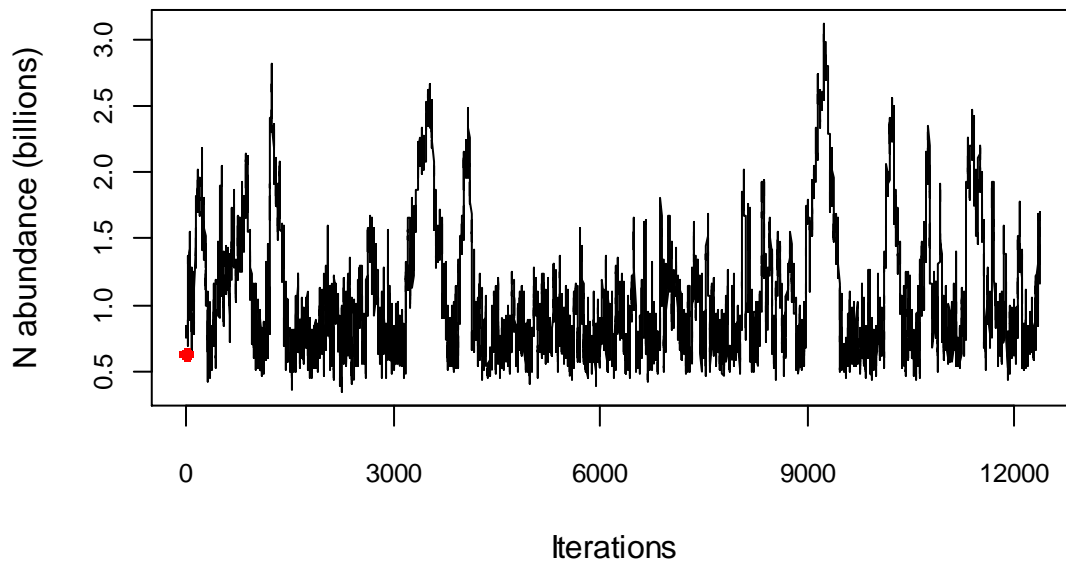


Figure A3 [previous page and above]. Markov Chain Monte Carlo iteration from the south sub-area Bayesian model, showing two alternating ‘states’ of low or high catchability coefficient q (top graph), with corresponding high or low N abundance (bottom graph). Horizontal gray line on the top graph shows the $q = 0.00035$ threshold line used to reject the low q state. Red dots on both graphs indicate the respective optimized values.

D. Expected individual *D. gahi* weight distributions

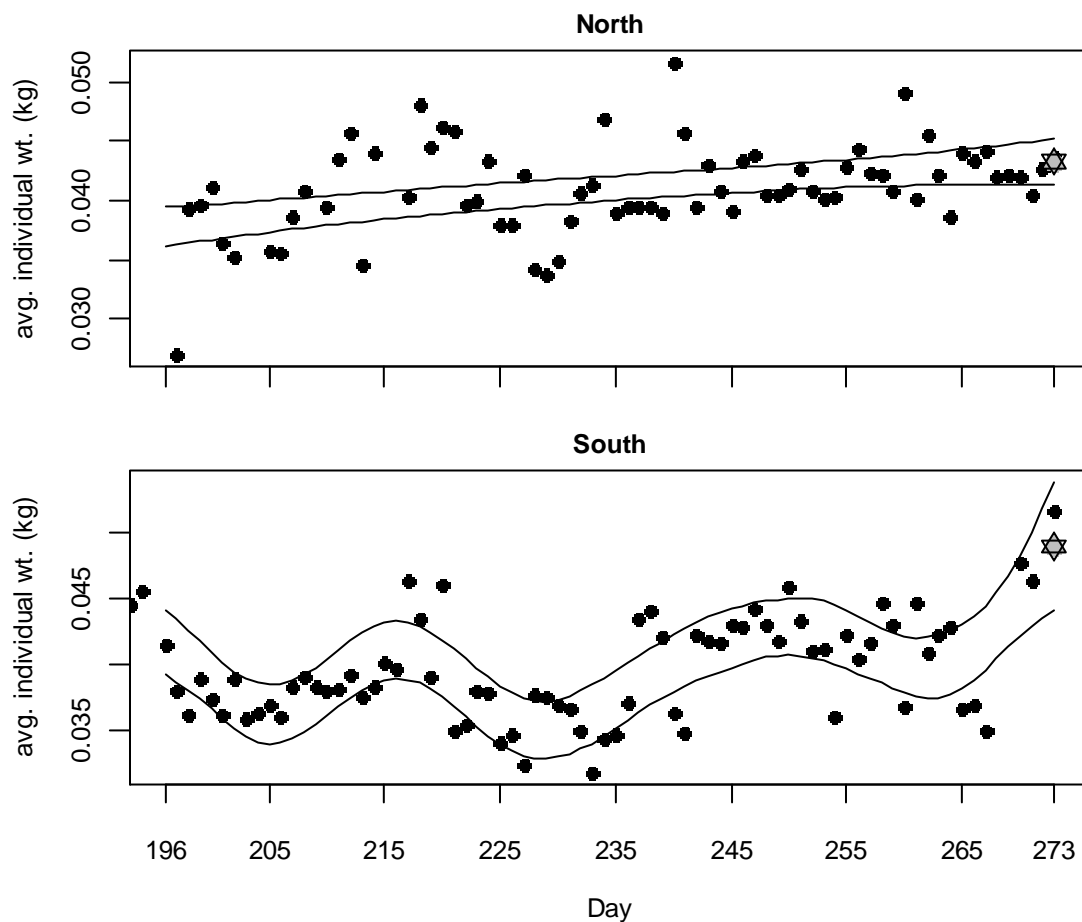


Figure A4 [previous page]. Daily average *D. gahi* weights (black points) and 95% confidence intervals of GAMs (black lines) of seasonal trend in average individual weight. Star symbols indicate the expected average weights on the modelled depletion period end days: $Wt_{N \text{ day } 273} = 43.3 \pm 1.0$ g (top), $Wt_{S \text{ day } 273} = 49.0 \pm 2.5$ g (bottom).